Advances in Geo-Energy Research

Vol. 2, No. 2, p. 122-134, 2018
www.astp-agr.com

Invited review

Recent advances on microscopic pore characteristics of low permeability sandstone reservoirs

Shengyu Huang[1*], Yiying Wu[2,3], Xiaobo Meng[4], Liwen Liu[5], Wei Ji[6]

[1]*No. 8 Oil Production Plant, PetroChina Changqing Oilfield Company, Xi'an 710018, P. R. China*

[2]*State Key Laboratory of Continental Dynamics of Ministry of Geology, Northwest University, Xi'an 710069, P. R. China*

[3]*Department of Geology, Northwest University, Xi'an 710069, P. R. China*

[4]*Unconventional Natural Gas Institute, China University of Petroleum, Beijing 102249, P. R. China*

[5]*Korla Branch of Bureau of Geophysical Prospecting Co., Ltd., CNPC, Korla 841001, P. R. China*

[6]*Changqing Division of China Petroleum Group logging Co., Ltd., Xi'an 710201, P. R. China*

(Received February 18, 2018; revised March 5, 2018; accepted March 6, 2018; available online March 10, 2018)

Citation:
Huang, S., Wu, Y., Meng, X., Liu, L., Ji, W. Recent advances on microscopic pore characteristics of low permeability sandstone reservoirs. *Advances in Geo-Energy Research*, 2018, 2(2): 122-134, doi: 10.26804/ager.2018.02.02.

Corresponding author:
*E-mail: corner090808@163.com

Keywords:
Microscopic pore characteristics
low permeability
sandstone
mercury
NMR

Abstract:
Understanding oil and gas production from low-permeability sandstones requires an understanding of the porosity. This paper reviews the analysis of data from hundreds of cores' microscopic pore characteristics of low-permeability sandstone reservoirs from Chang 6 reservoir of Ji-yuan oilfield in ordos basin. And this paper is to embody the methods used in the study of low permeable sandstone reservoir in recent years and the results reflected in it. For example, by analyzing the rock of Chang 6 reservoirs, it can be seen that the rock of Chang 6 reservoirs is mostly developed by Feldspar Sandstone, its internal pore types are diverse, the pore size is mainly small pore type, the second is fine pore, and has continuous spectral distribution, and the distribution is single peak shape. Different methods have been used to study low-permeability sandstones, including scanning electron microscope, casting thin plate, physical test means, high-pressure mercury, constant velocity mercury, NMR experiments. The results show that the pore-throat combination types of reservoir are mainly small pore-micro-larynx. The main type of reservoir throat is mainly flaky throat. The extremely strong heterogeneity in the layer is the key to the efficiency and effect of water flooding. Therefore, the exploration and development of low permeable sandstone reservoirs can be guided by the analysis of relevant parameters.

1. Introduction

With the rapid development of various undertakings in our country, the demand for oil is getting bigger and larger. China's Energy Development Report (December 2016) predicts that in 2016, China's oil apparent consumption is expected to reach 575 million tons a year, up 5.3% from 2015. Oil imports are expected to reach 375 million tons a year, up 11.7% from the previous year, and oil's external dependence could reach 65% percent (Yao et al., 2012). In 2017, China's crude oil apparent consumption reached 585 million tons, which grew 1.7% than 2016, and the domestic oil supply and demand contradictions further intensified. Low permeability and ultra-low permeability reservoirs are characterized by deposition, diagenesis, microscopic pore throat, macroscopic and microscopic heterogeneity, physical and chemical properties of fluids and other factors to control, making the development of the contradictions in the production and construction of the outstanding (Holditch, 2006), mainly manifested: the heterogeneity of the reservoir layer is strong, pore and throat radius small, capillary pressure is small, the oil-water seepage resistance is big, the oil-water distribution is complex, and the characteristic of the conventional reservoir is very different, the microscopic pore-throat network distribution pattern is very complicated, the pore throat type is diverse, the pore-throat coordination number is uneven, and the pore-throat connectivity is poor (Zou, 2013; Chen et al., 2017a). At the same time, the reservoir diagenesis and the differential distribution of micro-fractures cause low permeability, ultra-low permeability reservoir has relatively high permeability zone (Lin et al., 2017; Sidiq et al., 2017). Relying on traditional, single sedimentary control cannot explain the low permeability. In the development of ultra-low permeable reservoirs, only sedimentary, diagenesis

https://doi.org/10.26804/ager.2018.02.02.

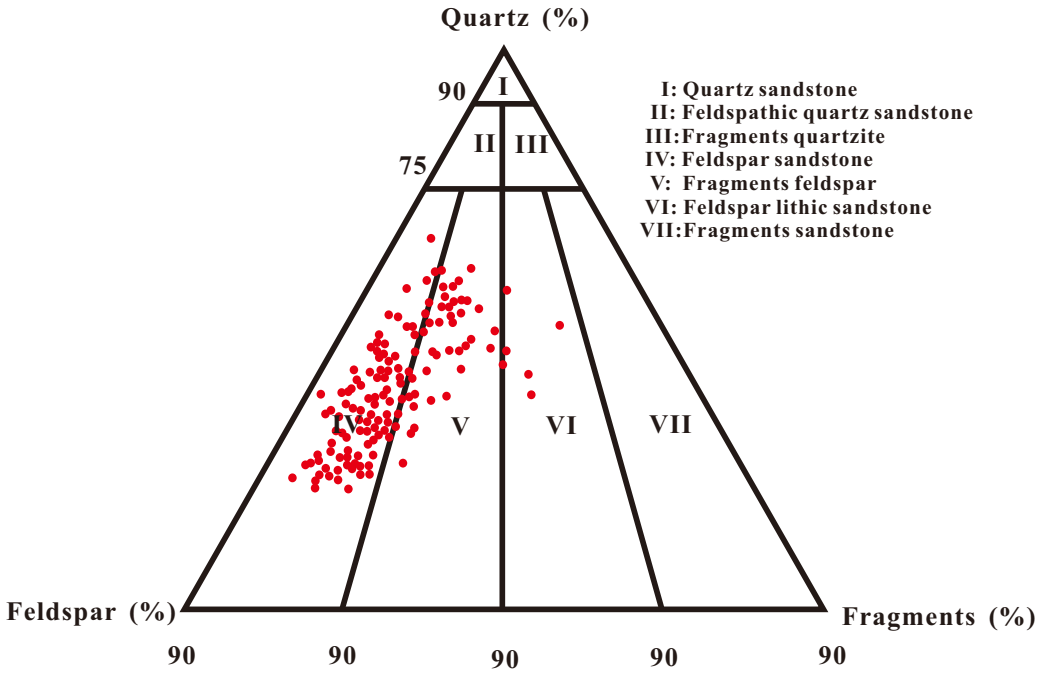

Fig. 1. The classification map of the Chang 6 reservoir sandstone in the Ji-yuan area.

and micro-pore structure characteristics can be combined to determine the basic characteristics of low-permeability reservoirs. So, the microscopic pore structure characteristics and seepage characteristics of low permeability and ultra-low permeable reservoirs are studied, which provides a reliable theoretical basis and technical support for the sustainable and efficient development of oil and gas reservoirs (Loucks et al., 2009).

The seepage characteristics of fluids in low permeability and ultra-low permeability reservoirs are different from the high permeability reservoir, and the whole Ordos basin is low permeability, ultra-low permeability reservoir, it is very important to study and understand the pore structure of low permeability, ultra-low permeability reservoir and the microscopic seepage characteristics and laws of fluids in reservoir (Nelson, 2009; Wang et al., 2017). Application of casting thin plate identification, scanning electron microscope, high pressure mercury, constant velocity mercury, oil-water phase infiltration, nuclear magnetic resonance and so on. These experiments are the main methods used for the microscopic pore characteristics of low permeable sandstone reservoir. This Paper, taking the Chang 6 reservoirs of Ji-yuan oilfield as an example, analyze the microscopic pore structure characteristics and microscopic seepage characteristics of Yanchang formation in Ordos Basin deeply. And this paper states the experimental results in order to introduce the research methods and results of microscopic pore characteristics study of low permeable sandstone reservoir in recent years briefly. The study shows that the pore types of 6 reservoir rocks mainly include intergranular pore, fragments micropore, micro-crack, etc. The main types of reservoir pore-throat combination are small pore-throat type, and other pore-throat combinations, such as small pore throat type, medium pore-throat type and so on. The type of reservoir throat is mainly lamellar throat, with necking and tube bundles in local development, and the pore-throat connectivity is medium. According to the results of constant velocity pressure mercury on the pore size distribution frequency, the pore radius of the study area is mainly distributed between the three peaks, the throat has a single peak shape and a multiple peak shape, mainly distributed between the two, and secondly, it shows that the reservoir throat distribution heterogeneity in the study area.

2. Method

2.1 Petrology research

The usual petrological study is based on the observation under the microscope of conventional thin plate and cast body, combined with SEM, cathode luminescence and X-ray diffraction (Loucks et al., 2009; Keller et al., 2011; Chalmers et al., 2012). This paper applied these methods to analyze the petrological characteristics of Chang 6 reservoirs synthetically, so as to introduce the achievements of petrology research for low permeable sandstone reservoir. In Chang 6, the content of reservoir feldspars and fragments is high; feldspar sandstone content is highest and most development; rock fragments feldspar sandstone content is second and other types are rare (Fig. 1).

According to several pieces of sandstone under the microscope identification, in study area of Chang 6, the composition of clastic are mainly feldspar and quartz whose absolute content is 10%~71% and average content is 38%.

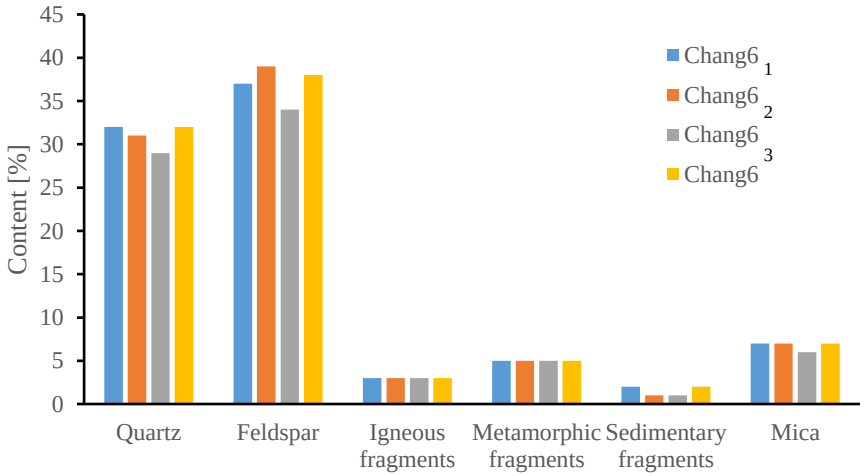

Fig. 2. The clastic composition and content of Chang 6 reservoirs in Ji-yuan area.

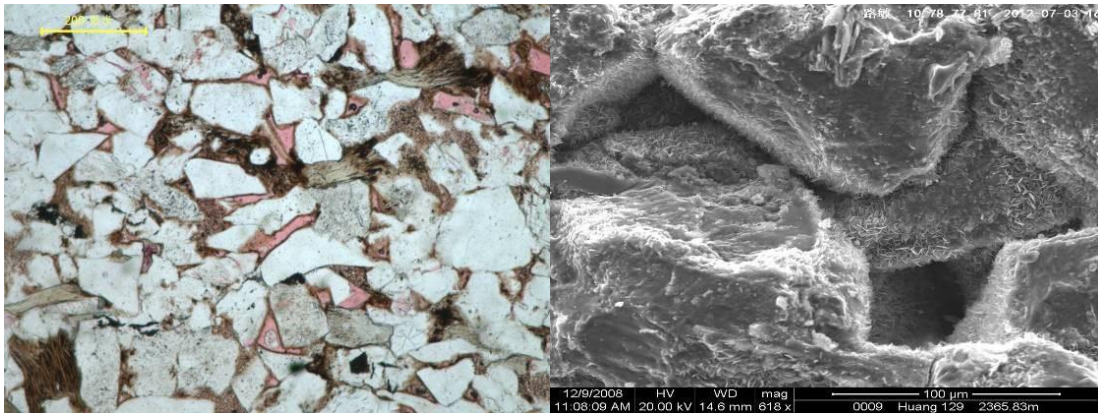

Fig. 3. The characteristics of the residual intergranular pores in the slab and the scanning electron microscope of the Chang 6 reservoir in the Ji-yuan area.

Quartz content is lower than feldspar content, absolute content 13%~70%, average 31.2%, rock fragments content is lowest, absolute content 0%~33.4%, the average content of 8.9%, which contain mostly metamorphic rock fragments, igneous fragments and less sedimentary fragments. The content of them is 5.1%, 2.4% and 1.3% respectively. The content of other clastic is mainly of mica, the general absolute content 0.0%~24.6%, the average content of 8%.

The content of the sandstone gap in Chang 6 reservoirs is relatively high, the absolute content of which is between 1%~39% and the average content of which is 13.32%, the content of cements is high, between 4%~39%. And the average content of it is 13.10%. The content of the impurity is low, which is between 0%~8.0%, and the average content is 2.29%. The main types of cements are iron calcite, kaolinite, chlorite, illite, calcite, silica, dolomite, iron dolomite, as well as a small number of mesh clay, feldspar, pyrite, siderite, and so on, the absolute content of which is 4.30%, 3.45%, 3.89%, 1.59%, 1.54%, 1.13%, 0.33%, 0.48%, 0.47%, 0.06%, 0.11% respectively. The analysis of the characteristics of the gaps in the small layers shows that kaolinite, chlorite, iron calcite, silica are high in content; the content of the impurity is less; kaolinite, chlorite and Fe-calcite are the highest in the reservoir rocks in the research area, and the development is common, the content of 6_3 small kaolinite, chlorite and Fe-calcite is obviously higher than that of Chang 6_1, 6_2 small layers. And the difference between the two content is small; illite and silica content are low. The content difference among Chang 6_1, Chang 6_2, Chang 6_3 small layer is not big (Fig. 2).

2.2 Pore type research

The study on the pore type of low permeable sandstone reservoir is based on the casting sheet and SEM date. According to the statistical analysis of them of the Chang 6 low permeable reservoirs in Ji-yuan area, the pore types of reservoir development in the research area include residual intergranular pores, feldspar, fragments soluble pores, intergranular pores, and a small number of micro-cracks, of which the residual intergranular pores, feldspar most developed, fragments dissolved pores, intergranular pores, the second, micro-fissure development of the least.

(1) Residual intergranular pore

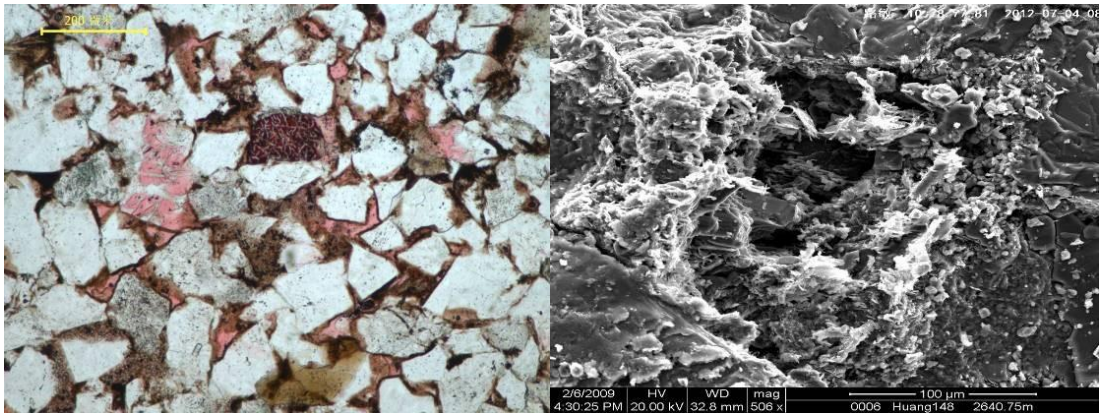

Fig. 4. The characteristics of feldspar pore in 6 reservoir slabs and scanning electron microscope of Ji-yuan area.

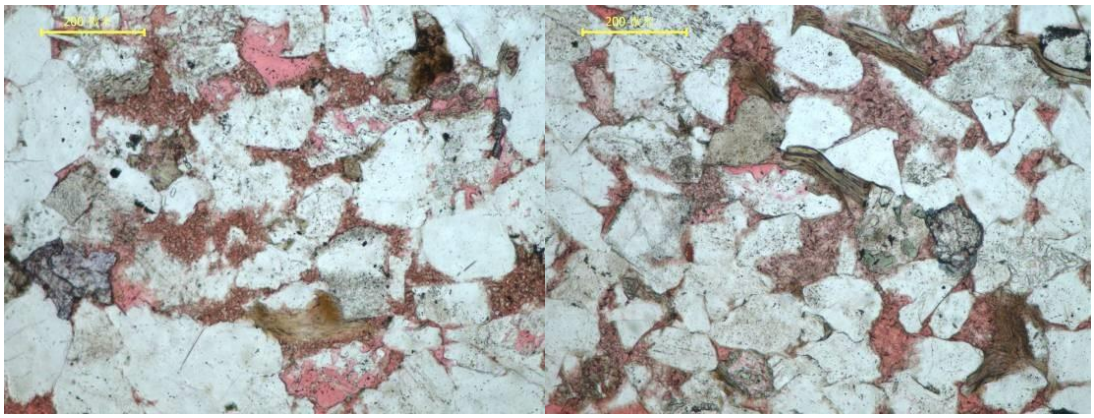

Fig. 5. The characteristics of fragments-dissolving holes in the Chang 6 reservoir slabs and scanning electron microscope of the Ji-yuan area.

Because of the compaction and late cementation in the early diagenesis, the loss of the original intergranular pores in the reservoir is serious, and only the pores which are not fully compacted and blocked are preserved (Zhou et al., 2011; Ji et al., 2016). The residual intergranular pore is located between the skeleton particle voids, the general shape is more regular, the size is different, and the Pore diameter is generally 50 μm$\sim$100 μm. According to the statistics of rock slices and scanning electron microscopy, the content of three small layers of residual intergranular pores in the study area is not significant (Fig. 3 and Fig. 8).

(2) Feldspar pore

The feldspar corrosion pores of Chang 6 low permeable reservoirs in Ji-yuan area are extremely developed. Feldspar generally along the cleavage joints and other soluble parts of dissolution, the rules of the cleavage, irregular honeycomb, or even feldspar particles are completely dissolved only to leave the particle shell, forming a mold hole. The pore Pore diameter is generally 10 μm$\sim$80 μm and can reach 100 μm, which contributes a lot to the reservoir performance and seepage ability of the research area, which is often associated with other pores and unevenly distributed. (Fig. 4 and Fig. 8).

(3) Fragments dissolving hole

The content of fragments dissolving hole is relatively high in the research area, which is an important reservoir space in the research area. It is formed by selective dissolution for acidic volcanic rock fragments soluble components. Pore diameter generally in 5 μm$\sim$30 μm, and the resolved large soluble pores can be visible by the naked eye, which distribution is very uneven (Fig. 5 and Fig. 8).

(4) Intergranular hole

Intergranular pores are more developed in Reservoir rock pores in the study area, mainly for the formation of kaolinite intergranular pores with better self-crystalline form, and also see illite and chlorite intergranular pores. In the study area, the intergranular pores of the reservoir are generally located between the crystalline and crystalline minerals. Although the contribution rate of intergranular pores to reservoir properties is generally, the capacity of reservoir seepage has a certain degree of contribution (Yang et al., 2014) (Fig. 6 and Fig. 8).

(5) Micro-cracks

Micro-cracks are usually formed under the action of compaction and other tectonic stresses (Lin et al., 2017; Sidiq et al., 2017). And the micro-cracks have less content in the pores of 6 reservoirs in the Ji-yuan area, but the local area can reach 1.2%$\sim$2.0%. Although the content of micro-cracks is not much, they can communicate the original disconnected pores. That is why they can greatly improve the reservoir seepage capacity (Fig. 7 and Fig. 8).

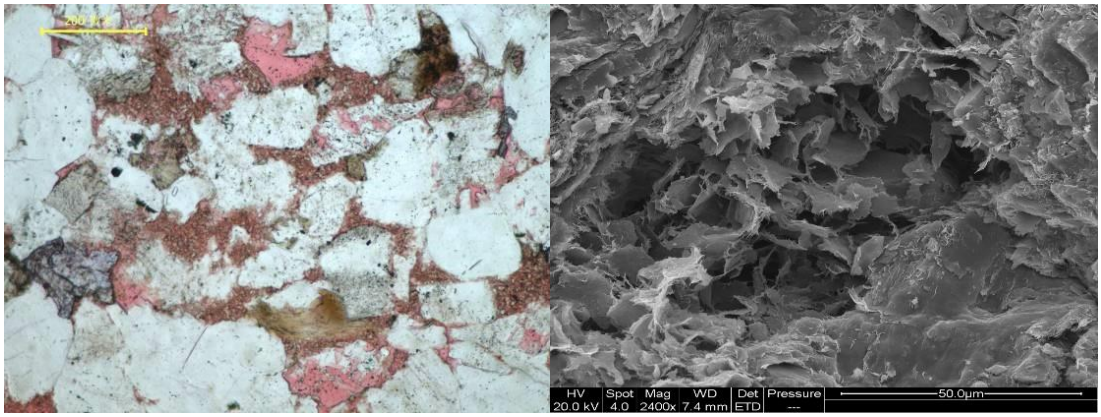

Fig. 6. The characteristics of the intergranular pore in the cast thin plate and scanning electron microscope of the Chang 6 reservoir in the Ji-yuan area.

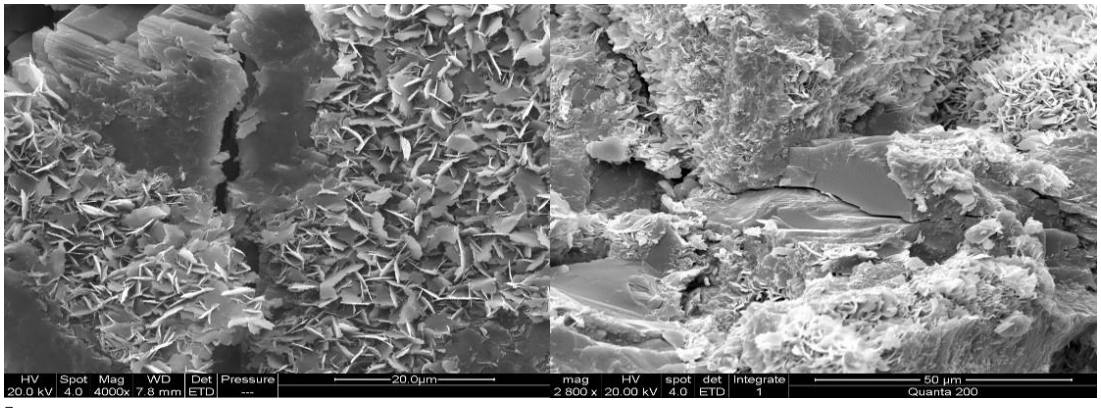

Fig. 7. The characteristics of the micro-fissure of the Chang 6 reservoirs in the Ji-yuan area.

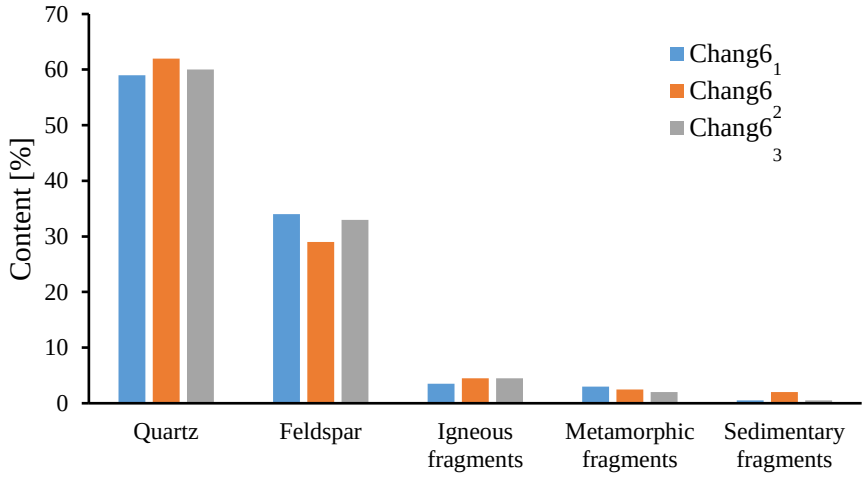

Fig. 8. The statistical Chart of pore types and contents of Chang 6 reservoir in Ji-yuan area.

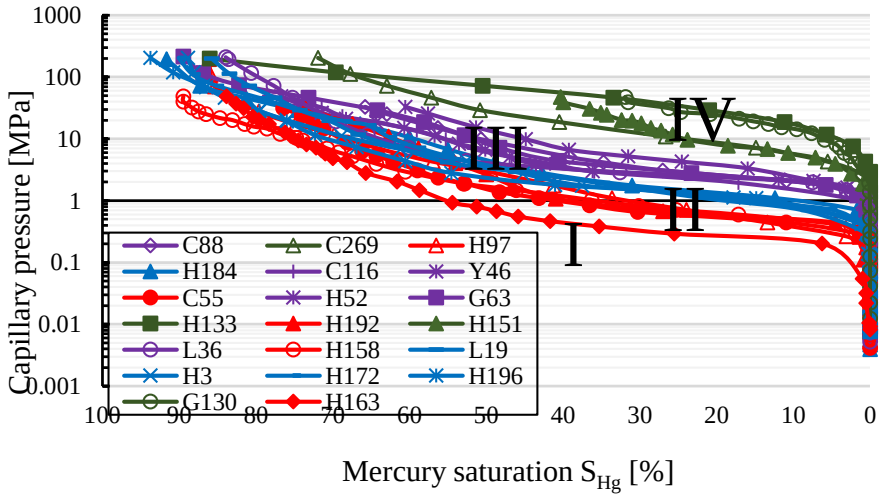

Fig. 9. Classification of capillary pressure curves of 6 reservoir rock samples in Ji-yuan area.

2.3 Capillary pressure mercury technology characterizing microscopic pore throat characteristics

Capillary pressure method is also an effective method for laboratory indirect study of microscopic pore structure (Keller et al., 2011). The capillary pressure method is developed on the basis of the research methods of casting thin plate and scanning electron microscope, and compared with the casting thin plate and SEM, the capillary pressure mercury has its own superiority, so it is used by many scholars to indirectly determine the pore throat characteristic of the reservoir (Ross et al., 2009; Huang et al., 2018b).

According to the study of Chang 6 Reservoir's 35 samples (6_1 small layer 14 samples, Chang 6_2 small layers 9 samples and Chang 6_3 small layers 12 samples), the representative of the rock sample mercury data and the corresponding capillary pressure curve analysis show: displacement pressure, pore throat distribution distortion, separation and maximum mercury saturation are the main factors to control the formation of capillary pressure curve. According to these parameters and the corresponding capillary pressure curves, the capillary pressure curves in the study area are divided into four types (Zhang et al., 2015), such as I, II, III, IV and V (Fig. 9).

The distribution of capillary curve types in Chang 6 reservoir shows that the types of II and III-type capillary pressure curves are the most common, and I and IV are relatively rare. The Chang 6_1 small layer is mainly II class (64.3%), the second is I class (21.4%) and the third is III Class (14.3%), there is no IV class, 6_2 small Layer II class (55.6%) is the largest proportion, the proportion of the difference between III (22.8%) and IV (21.6%) is not, no I class. And II class (41.7%) and III class (41.7%) curves are the most common in the Chang 6_3, the follow is IV class (16.7%), and there is no I class. The results indicated that the concentration of the 6_1 small-layer pore throat was good, and the reservoir performance and seepage ability are the best. The 6_2 small-layer pore throat distribution is good, and its reservoir performance and seepage ability are worse than Chang 6_1 small layer. The Chang 6_3 small pore throat distribution is general, and its reservoir performance and seepage ability are worse than Chang 6_2 small layer.

2.4 Characterization of microscopic pore-throat characteristics by constant-velocity mercury injection technique

The constant-velocity mercury injection technique is an important method for the study of low permeable sandstone reservoir in recent years. J.I. Gates as early as 1959, the pressure fluctuation was observed in the determination of Karst cave type carbonate samples by Mercury-pore analyzer in the interior. In 1966, Crawford and Hoover recorded pressure fluctuations in the process of injecting water into man-made porous media (Crawford et al., 1966); in 1970, in this paper, the morrow of the wetting phase is discussed in detail, and some terms are introduced to describe the pressure fluctuation characteristics (Morrow, 1970). In 1971, Gaulier also sent similar experimental technical articles, but the test accuracy was low (Higgs et al., 2007; Sheng et al., 2017). The real application of the constant velocity Mercury test is Yuan and Swanson. They first developed at apex of the pore Analyzer APEX (Apparatus for pore examination) (Yuan et al., 1989). The key equipment is the automatic data acquisition system which is combined with high resolution pressure measurement. The experiment was to inject mercury into porous media at very small velocities, assuming that the contact and interfacial tension in the injection process remained unchanged, providing detailed information on pore space structures by monitoring the pressure fluctuations of the mercury during injection (Huang et al., 2018b).

Fig. 10 is a schematic diagram of the hole, throat group and mercury fluid breaking through the pore and throat. Fig. 11 is the curve of the volume of mercury in the pressure fluctuation recorded during mercury injection. When the mercury first enters the main throat, the pressure gradually rises to a certain

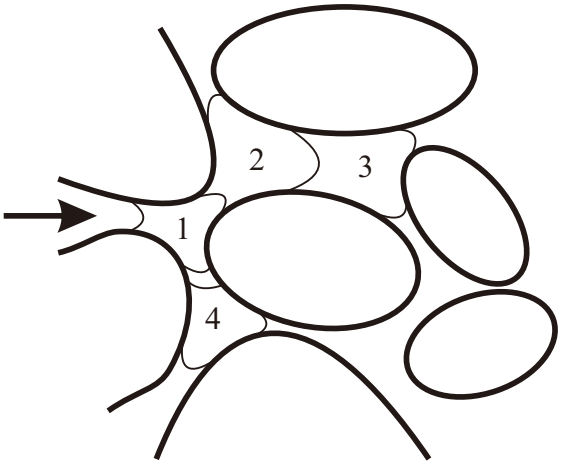

Fig. 10. Schematic diagram of pore structure of constant velocity mercury pressure.

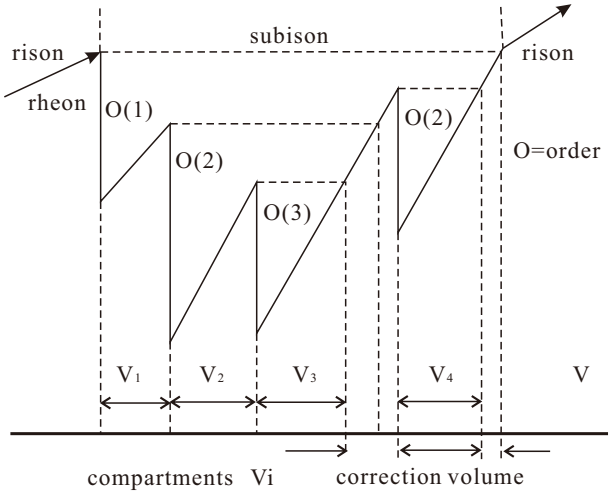

Fig. 11. Schematic diagram of constant velocity mercury pressure.

value. Then the mercury breaks through the throat into the pore 1, and the pressure drops. As shown in Fig. 11, the first pressure drops $O_{(1)}$. Mercury gradually fills the pore 1 after the pressure picks up, mercury enters the next secondary throat. Mercury breaks through the throat into the pore 2, then the pressure is lowered again, resulting in a second secondary pressure landing $O_{(2)}$. And so on, mercury gradually fills all the pores controlled by the main throat until the pressure rises to the pressure at the main throat, which is a complete pore throat unit. The main throat radius is determined by the pressure of the breakthrough point, and the pore size is determined by the volume of Mercury. The throat size and quantity can be clearly reflected in the mercury injection pressure curve.

The local pressure characteristic curve and capillary pressure curve of rock sample can be obtained by constant velocity Mercury experiment, which plays an irreplaceable role in obtaining the data of constant velocity mercury. By analyzing the local pressure curve recorded during the constant velocity Mercury experiment, the effective throat and effective pores in the rock samples can be separated, and the number of effective throat and effective pores is obtained accurately. Based on the analysis of local pressure curve, the three capillary pressure curves of total pore throat, effective throat and effective pore were obtained by constant velocity mercury pressure experiment.

The constant velocity mercury test directly gives the capillary pressure curve of the total pore throat, the pore capillary pressure curve, and the capillary pressure curve of the throat, which reflect the microscopic pore-throat characteristics of the sample and the characteristic parameters of the microstructure. The characteristics of microscopic pore and throat were comprehensively analyzed from the characteristics of throat distribution, pore distribution and the distribution of pore throat ratio.

Through our example, the experimental samples can be divided into three categories: I class, 1th sample throat radius of the main distribution range of 0.5 μm$\sim$1.2 μm; II class, 3, 4, 5th samples throat radius of the main distribution range is 0.3 μm$\sim$1.1 μm; III class, 2, 6th sample throat radius of the main distribution range is 0.3 μm$\sim$0.7 μm. Overall the Chang 6_1 small-layer experimental sample throat is wider than 6_2 small layer of experimental sample throat thick.

2.5 Characterization of microscopic seepage flow by NMR technique

Nuclear magnetic resonance (NMR) as a physical phenomenon in which nuclei in a magnetic field absorb and re-emit electromagnetic radiation, in 1946 by the Harvard University of Purcell and Stanford University of Bloch two individuals independently found. In the 1956, Brown and Fatt studies found that when the fluid was in the pores of the rock, the NMR relaxation time was significantly reduced compared with the Free State. In order to find the cause of this phenomenon, a lot of experiments and theoretical studies have been carried out to find that the magnetic resonance relaxation time of fluids is related to the pore size of the environment. The NMR relaxation theory of rock porous media was proposed by Brownstein and Tarr in 1979. Nowadays, NMR technology has been widely used in core analysis and log analysis, and it plays an important role in the study of oil and gas reservoirs (Ausbrooks et al., 1999; Yao et al., 2010; Meng et al., 2016).

When the fluid (oil, gas, water, etc.) saturated into the pore of the rock sample, the fluid molecule will be subjected to the pore solid surface force, and the force depends on the size of the pore (pore size, pore shape), minerals (mineral composition, mineral surface properties) and fluid (fluid type, fluid viscosity) and so on (Coates et al., 1999). In the NMR, when the rock samples of saturated fluids (water or oil) were measured, the amount of T_2 relaxation time depends on the strength of the fluid molecule by the surface force of the pore. So, the T_2 relaxation time is the reflection about the pore size, pore shape, mineral (mineral composition, mineral surface property) and fluid (fluid type, fluid viscosity, and so

on). By using the NMR T_2 relaxation time and its distribution characteristics of the fluid in rock samples, the occurrence state of the fluid in the pore of rock samples can be analyzed (Ge et al., 2011). When the fluid is subjected to a strong force on the pore solid surface (such as a fluid in a small pore or a fluid close to the solid surface in a larger pore), the T_2 relaxation time of the fluid is small, which means the fluid is in a bound or inactive state and it is called a bound or incompressible fluid. Conversely, when the fluid is weakened by the force of the pore solid surface (such as a fluid that is not tightly contacting the solid surface in larger pores), the fluid T_2 relaxation time is large, which means the fluid is in the free or movable state, and it is called free fluid or movable fluid. At this time, the corresponding saturation is the movable fluid saturation (Ausbrooks et al., 1999; Mai et al., 2002; Yao et al., 2010).

To sum up, the irreducible fluid and the movable fluid in the core pores are obviously different in the NMR T_2 relaxation time. Therefore, NMR T_2 spectra can be used to analyze the state of occurrence (movable or restrained) of the salt water in the core pores, and the saturation of the movable fluid and the irreducible fluid saturation are given quantitatively (Lonnes et al., 2003; Martin et al., 2004).

The boundary value of the movable fluid and the incompressible fluid is 13.895 ms in the NMR experiment T_2 (Coates et al., 1999; Westphal et al., 2005), and the movable fluid is on the right side, the left is the incompressible fluid. Generally, we think that the total fluid of the movable fluid is the movable fluid saturation (Hamada et al., 2002; Hossain et al., 2011).

The results of NMR often reflect a lot of problems, and we show it through an example. According to Table 1, Fig. 12 Experimental Sample analysis test results and T_2 diagram analysis know:

1th sample fluid saturation is 63.3%, porosity is 11.8%, permeability is 0.555×10^{-3} μm^2, the spectral map is bimodal, the right peak area is obviously greater than left peak, and the main peak is located on the right side of 13.895 ms, the dynamic fluid saturation is high, which indicates that the fluid in the pores is the majority. According to the experimental analysis of conventional physical property, rock Flake, SEM, high pressure mercury and constant velocity mercury, it is found that the sample has the advantages of large porosity, thick throat, good connectivity of pore and throat, but small pore throat. The fluid saturation of the 2nd sample is 31.74%, the porosity is 9.67%, the permeability is 0.052×10^{-3} μm^2, the spectral map is bimodal, the right peak area is obviously less than left peak, the main peak is located on the left side of 13.895 ms, the fluid saturation is low, which indicates that the irreducible fluid in rock samples is the most and the movable fluid content is less. The sample pore throat is more developed, the large pore throat develops generally, the connectivity is good, but the particle sorting is general and the size is mixed. 3rd Sample Fluid saturation is 28.41%, porosity is 13.54%, permeability is 0.140×10^{-3} μm^2. And it is similar to 2nd sample spectra, 3rd Sample has bimodal. But the difference is that the proportion of large pore throat is less than 2nd sample and the saturation of movable fluid is low. 4th Sample Fluid saturation is 21.95%, porosity is 16.91%, permeability is 0.216×10^{-3} μm^2, and the spectral map is single peak. The maximum is at the left of T_2 boundary value, the fluid saturation is very low, which indicates that the bound fluid occupies a large proportion of pore space. The microscopic observation shows that the small pores and fine throat are generally developed, and the large pore throat is rare, but the granules are well selected. The fluid saturation of the 5th sample is 25.92%, porosity is 12.9%, permeability is 0.209×10^{-3} μm^2, and the spectrum is bimodal, the difference between the left and right peak area is small, the left peak is slightly greater than the right-hand peak. The main peak is located on the left side of the boundary value, and the movable fluid saturation is low, which means the movable fluid occupies the volume space is not high. The pore throat in 5th is common, the pore throat is undeveloped, and the particle sorting is better. The 6th sample fluid saturation is 40.12%, its porosity is 12.75% and permeability is 0.292×10^{-3} μm^2. The spectral map in the 6th sample is bimodal, and the left and right peak area is not big, which means the movable fluid saturation is high and the fluid content in the pore flow is more. The pore volume ratio of the large pore throat is larger than that of the pore throat, which is generally connected well, but its particle sorting is general.

Table 1. Criteria for evaluating the saturation of NMR movable fluids.

Saturation of movable fluid /%	Reservoir classification
> 65	Class I (Good)
$50 \sim 65$	Class II (Better)
$50 \sim 65$	Class II (Better)
$35 \sim 50$	Class III (Medium)
$20 \sim 35$	Class IV (Poor)
< 20	Class V (Very poor)

The geological conditions of reservoirs, especially low-permeability reservoirs, are complex. They have small pore size, big surfaces, different clay type, different content and vary greatly saturation degree of movable fluid, so the reservoir evaluation, especially the low permeability reservoir evaluation, should consider the parameters of hydrodynamic saturation. According to the experience of oil and gas field development and production at home and abroad, if only the saturation of movable fluid is the standard, the reservoir difference can be divided into five categories (Table 1).

This study applies the standard to the actual sample. It can be seen from table 2 that the fluid saturation of 1th and 6th fluids are high and their pores are large, their throats are thick, their fluid seepage resistance are small. The 2nd, 3rd, 4th, 5th samples fluid saturation are smaller in order, their fluid saturation are low (mostly less than 30%), their pore size are mixed, their throat bend are deformed, the fluid seepage resistance in them are big, and their bound fluid

Table 2. Experimental results of constant velocity mercury pressure in 6 reservoirs in Ji-yuan area data table.

No.	Effective Pore Volume ml/cm^3	Effective throat Volume ml/cm^3	Number of throat channel per unit volume cm^3	Number of pores per unit volume cm^3	Weighted average value of pore radius μm	Weighted average value of throat radius μm
1	0.1476	0.0866	4718	4718	130.94	0.886
2	0.0655	0.0786	2078	2076	135.28	0.428
3	0.0984	0.0859	3905	3902	129.79	0.574
4	0.0946	0.0904	4701	4697	127.74	0.582
5	0.1189	0.0719	4749	4742	129.58	0.687
6	0.1039	0.0671	4299	4296	129.20	0.635
7	0.0040	0.0280	278	278	116.85	0.501

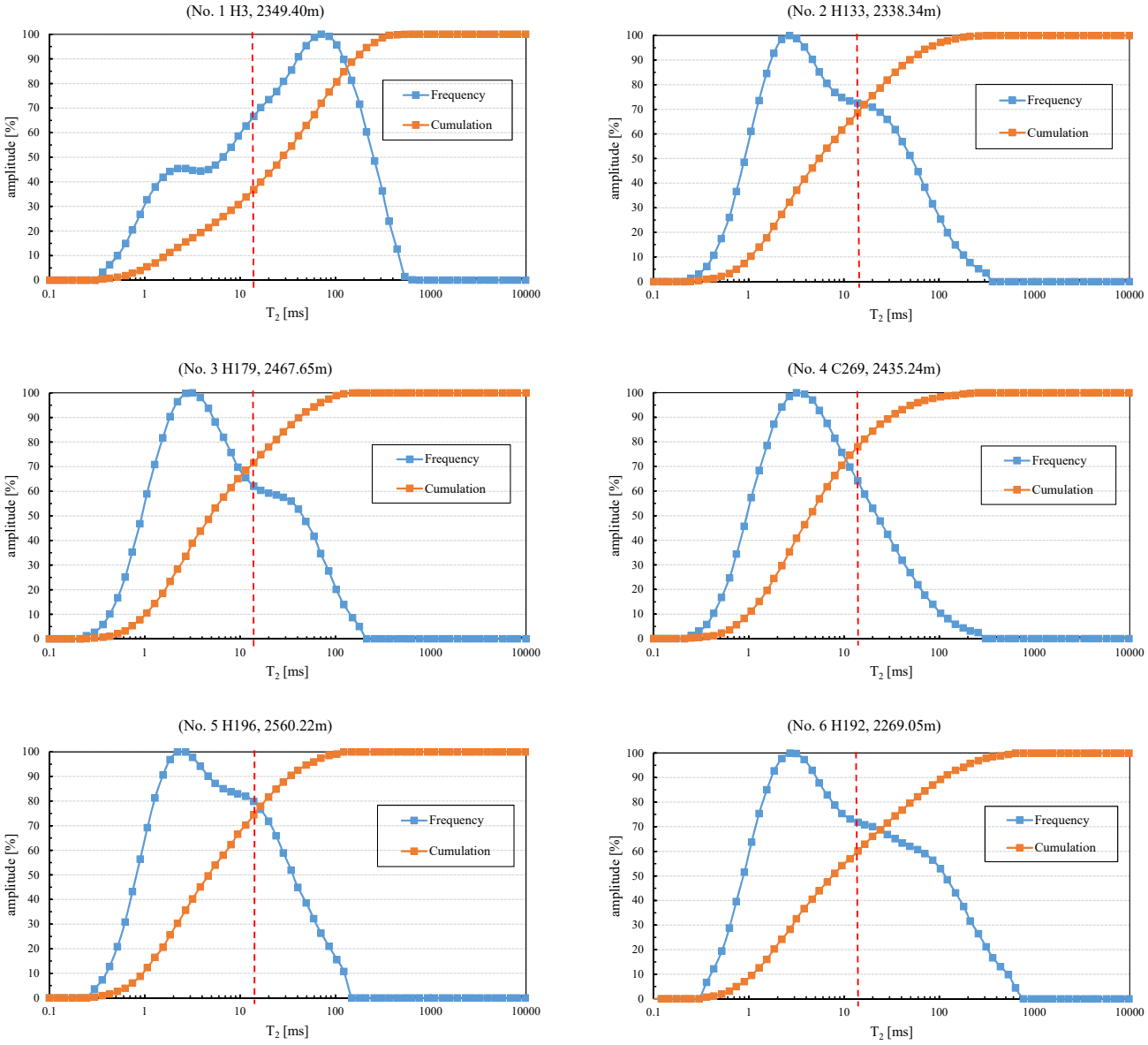

Fig. 12. The frequency distribution and cumulative distribution of NMR T_2 spectra in the saturated water state of Chang 6 reservoir samples in the Ji-yuan area.

content are high. According to the previous use of dynamic fluid saturation of reservoir classification criteria, 6 NMR experimental samples in the study area were classified, of which 1th sample belonged to (50%∼65%), which was better reservoir, the 6th sample belonged to (35%∼50%), medium reservoir, and the 2nd, 3rd, 4th and 5th samples belonged to class (20%∼35%) are poor reservoirs.

3. Recent developments and extensions

In the study of Petroliferous Reservoir, it is found that the study of pore structure is the core of reservoir microscopic physics research. The pore structure of reservoir mainly refers to the relationship among the pore type, the throat type and pore geometry shape, size, distribution, interconnection. And they are also the overall appearance of reservoir pore development (Zha et al., 2017) and the important factors in determining fluid flow and hydrocarbon migration in reservoirs (Huang et al., 2017). For us, the deep study of reservoir pore structure will help us to fully understand the production capacity of oil and gas reservoir, and it will play a certain role in improving oil and gas recovery in the later development process (Li et al., 2017b). At present, the research methods of reservoir pore structure include: (1) the pore and throat of the reservoir are determined by the determination of capillary pressure; (2) the pore structure and the mineral composition of the reservoir are analyzed by the of the casting thin plate; (3) the SEM technique to analyze the mineral types and to understand the microscopic pore structure characteristics; (4) the pore characteristics such as pore structure, pore connectivity and throat distribution are studied by using the technology of mercury injection. The combination of the above methods can help us to understand the pore structure of reservoir in the research area more intuitively and comprehensively.

A large number of studies have shown that the pore types of low permeability and ultra-low permeability reservoirs mainly include intergranular pores, dissolution pores, microporous pores, intergranular pores, micro-fissures, and so on, among which mainly small and medium pores (Chen et al., 2017a). According to the previous research, it is concluded that in the ultra-low permeability reservoir, intergranular pores are in the pores in the form of residual intergranular pores, and in the number, which may be less than the dissolution pore, but in the porosity, which is mainly the intergranular pore. The type of pore is mainly dissolved pores, intergranular, dissolved pore type, micro-pore type mainly. The main types of laryngeal type are pore type, necking type, flake shape, point shape, tube bundle type throat, and the main types of orifice and throat combination are medium-pore capillary type, small-pore-throat type and micro-pore, micro-throat and micro-fissure mixed type. Heng Henwen, etc. through the study that: triangles, the pores of quadrilateral, polygon and long type are more developed in the sandstone reservoir with more developed pores, while the pores of the peak fossa, the long hole and the star point shape are more developed in the sandstone reservoirs with higher content of mudstone, siltstone, fine sandstone and more diagenesis. It has been found that the pore system with small Pore diameter type, micro-pore type, fine throat type and micro-throat combination is very complex in these reservoirs, which will bring great difficulties to oilfield development in the process of production (Li et al., 2017a).

The study of microscopic pore-throat structure in foreign countries originated from the 1930 s. Entering the 1970 s, due to the actual production needs, China has set off the first peak of micro-pore-throat field, some research areas have made breakthroughs. Entering the 1980 s, some of our scholars work in the integration of relevant theory and methods. Entering the 2000 s, the current micro-pore throat structure of the research field has made breakthrough progress, and a new era of micron-one nanometer, multi parameter call and model calibration is started.

In the early stage, the experimental methods were limited to the experimental statistical methods, based on the use of cast thin slices, scanning electron microscope, image porosity, diffraction and conventional pressure degrees, the microscopic pore-throat characteristics were quantitatively described. But the relationship between the different experiments was not enough, and the quantitative characterization of the micro-coupling mechanism with multiple experiments and multi-scale was not involved. The traditional casting sheet can only carry on the semi-quantitative analysis to the pore structure characteristic in the core sheet, such as pore shape and diameter, throat shape and diameter, face rate, pore throat coordination number, and this method is mainly based on the point-counting method to statistic. The development process of SEM technology: the traditional SEM can only qualitatively describe the conditions in the pores and the basic characteristics of clay and cementation. With the continuous application of analytical testing techniques such as medicine and materials science in the field of petroleum exploration and development, high-resolution field emission scanning electron microscopy (SEM) can be used to study the nanometer porosity of tight hydrocarbon reservoir and shale gas reservoir, and it can be found that the nanometer pore diameter is less than 1m, which changes the distribution range of the traditional reservoir pore throat (Blunt et al., 2013). The target of oil and gas exploration and development is increased. With the use of scanning confocal microscope, the image scanned by the cast thin slices can be reconstructed, and the three-dimensional image of the rock structure feature is obtained, which greatly weakens the cutting effect of the two-dimensional slice.

In the latter part, the multidisciplinary and quantitative calibration was used to combine the NMR, the constant velocity mercury, the traditional experimental means of the progress, and some other physical models, which could reflect the microscopic pore-throat characteristics. The application of NMR technology has its unique advantages in the study of pore structure, and the T_2 spectra drawn by NMR technology can not only quantitatively demarcate the micro-flow pore throat of the reservoir by using T_2 cutoff value, but also obtain two characteristic parameters of dynamic fluid saturation and movable flow porosity. These two characteristic parameters are the comprehensive reflection of the macroscopic and microscopic characteristics of the reservoir.

Later, the related pore structure theory model is developed, which includes two micro-model methods, namely fractal

model and network model (Yang et al., 2015, 2016; An et al., 2016; Huang et al., 2018a). Fractal refers to those specific geometrical form which is not obvious, but the overall has a certain similarity of the graph, structure and phenomenon of the general name, here refers to the pore shape. And the dimension is to characterize the pore shape in space complexity (Yu et al., 2009; Liu et al., 2016; Wei et al., 2017). The fractal geometry model is characterized by the high complexity of porous media, pore structure and pore throat distribution which have similar fractal characteristics. The fractal dimension method cannot establish a real model, but first of all, using the basic data, such as NMR T_2 spectral distribution, to derive a fractal dimension of the pore structure of the expression. The different pores are differentiated by the expression, or the fractal dimension of pore structure and the probability density distribution of pore throat radius are calculated according to the capillary pressure curve data (Mandelbrot, 1975; Yu et al., 2009; Cai et al., 2010; Huang et al., 2018a). Another network model is studied by means of mathematical deduction based on the assumption that microscopic pores are isolated plates, spheres and tubular pores. Assuming that the spherical tube model is used, the pore of the rock is spherical and the throat is tubular. The rock pores are grouped first, and the spherical tube model is used in each group, and the pore of the rock is divided into Mau and spherical holes, and then the numerical analysis method is employed to study it. The advantage of this method is that it can visually observe the spatial geometry distribution of the pore in the core, and can reflect the formation information (Zhang et al., 2017). The emerging digital core technology is a method of establishing the network model, which is based on the microscopic test method to obtain the pore space distribution and the particle structure inside the core by computer simulation (Yang et al., 2015, 2016; An et al., 2016; Chen et al., 2017b). Through the establishment of fractal model or network model and the combination of conventional experimental analysis and advanced constant speed and nuclear magnetic experiment, it is of great significance to deeply analyze the microscopic pore-throat structure of low permeability and ultra-low permeable reservoir.

The seepage characteristics of fluids in reservoir pores mainly depend on the nature of reservoir fluids, the properties of pore structure and the interaction between pore and liquid in reservoir. According to the Oil field production practice, the seepage characteristics of low permeability and ultra-low permeability reservoir are completely different from those of middle and high permeable reservoirs. At present, the understanding of the seepage characteristics of the middle and high permeable reservoirs has been more in-depth and the theoretical level is already very high, but there is still a lack of in-depth understanding of the characteristics of seepage in low permeability and ultra-low permeability reservoirs.

The future development trend is based on the quantitative classification of microscopic pore and throat structure, and combined with various experimental methods and seepage theory, in-depth analysis of the unique micro-seepage mechanism of low permeability and ultra-low permeability reservoir. In order to effectively improve the overall benefit of low permeability and ultra-low permeability reservoirs in the process of development, and solve the problems encountered in the development process, it is necessary to study the microscopic pore structure and microscopic water displacement characteristics of low permeability and ultra-low permeability reservoir, and study the storage and migration ability of oil and water in different pore types. As well as the study of oil and water seepage law, by analyzing the influence of these factors in the process of oilfield development, we can make it easier to recognize the low permeability and ultra-low permeability reservoir from the reservoir mechanism and essence, and also to solve the problems encountered in the process of water injection development.

4. Conclusion

From numerous studies of low permeable sandstones throughout the Chang 6 reservoir of Ji-yuan oilfield the following conclusions concerning pore structure and microscopic seepage characteristics of low-permeability sandstones seem apparent:

Because of the complex relationship of low permeable sandstone reservoir distribution, pore throat distribution and the diversity of oil-water micro seepage mechanism, low oil displacement efficiency, the development of contradiction, we need some specific experimental analysis methods to figure out the favorable area under the background of complex dessert. At present, with the help of scanning electron microscope, casting thin section, physical test, high-pressure mercury injection, constant velocity mercury injection and NMR, we both indirectly and directly study the petrological characteristics, pore-throat structure and seepage characteristics of low permeable sandstone reservoir from. We figure out the mineral composition, pore and throat type, pore and throat size, pore throat assemblage characteristics and physical parameters of reservoir, further to analyze the pore throat feature parameters and the effect of pore throat size distribution on the properties and seepage ability, so as to cast light on the target area and horizon for exploration and development in this tight reservoir with very strong heterogeneity.

Acknowledgments

This work was supported by the Natural Science Foundation Research Project of Shaanxi Province (2016JQ4022) and the Shaanxi Province Science and Technology Co-ordination and Innovation Engineering Project (2011KTZB01-04-01). The authors sincerely thank the Changqing Oilfield Company of PetroChina Co. Ltd. for providing the drill cores used in this study.

References

An, S., Yao, J., Yang, Y., et al. Influence of pore structure parameters on flow characteristics based on a digital rock and the pore network model. J. Nat. Gas Sci. Eng. 2016, 31: 156-163.

Ausbrooks, R., Hurley, N.F., May, A., et al. Pore-size distributions in vuggy carbonates from core images, NMR, and capillary pressure. Paper SPE56506 Presented at SPE annual technical conference and exhibition, Houston, Texas, 3-6 October, 1999.

Blunt, M.J., Bijeljic, B., Hu, D., et al. Pore-scale imaging and modelling. Adv. Water Resour. 2013, 51(1): 197-216.

Cai, J., Yu, B., Zou M., et al. Fractal characterization of spontaneous co-current imbibition in porous media. Energy Fuel 2010, 24(3): 1860-1867.

Chalmers, G., Bustin, R., Power, I. Characterization of gas shale pore systems by porosimetry, pycnometry, surface area, and field emission scanning electron microscopy transmission electron microscopy image analyses: Examples from the Barnett, Woodford, Haynesville, Marcellus, and Doig units. AAPG Bull. 2012, 96(6): 1099-1119.

Chen, L., Jiang, Z., Liu, K., et al. Quantitative characterization of micropore structure for organic-rich lower silurian shale in the Upper Yangtze Platform, South China: Implications for shale gas adsorption capacity. Adv. Geo-energ. Res. 2017a, 1(2): 112-123.

Chen, X., Zhou, Y. Applications of digital core analysis and hydraulic ow units in petrophysical characterization. Adv. Geo-energ. Res. 2017b, 1(1): 18-30.

Coates, G.R., Xiao, L., Prammer, M.G. NMR logging: principles and applications. Haliburton Energy Services, Houston, 1999.

Crawford, F.W., Hoover, G.M. Flow of fluids through porous mediums. J. Geophys. Res. 1966, 71(12): 2911-2917.

Ge, X., Fan, Y., Zhu, X., et al. Determination of nuclear magnetic resonance T_2 cutoff value based on multifractal theoryAn application in sandstone with complex pore structure. Geophysics 2014, 80(1): D11-D21.

Hamada, G.M., Awad, M.N.A. Evaluation of low resistivity beds using nuclear magnetic resonance log. J. King Abdulaziz Univ., Eng. 2002, 14(1): 47-61.

Higgs, K.E., Zwingmann, H., Reyes, A. G., et al. Diagenesis, porosity evolution, and petroleum emplacement in tight gas reservoirs, Taranaki basin, New Zealand. J. Sediment Res. 2007, 77(12): 1003-1025.

Holditch, S. A. Tight gas sands. J. Pet. Technol. 2006, 58(6): 86-93.

Hossain, Z., Grattoni, C.A., Solymar, M., et al. Petrophysical properties of greensand as predicted from NMR measurements. Pet. Geosci. 2011, 17(2): 111-125.

Huang, H., Chen, L., Sun, W., et al. Pore-throat structure and fractal characteristics of Shihezi formation tight gas sandstones in the Ordos Basin, China. Fractals 2018a, 26(2): 1840005.

Huang, H., Sun, W., Ji, W., et al. Effects of pore-throat structure on gas permeability in the tight sandstone reservoirs of the Upper Triassic Yanchang formation in the Western Ordos Basin, China. J. Pet. Sci. Eng. 2018b, 162: 602-616.

Huang, Z., Zhang, X., Yao, J., et al. Non-Darcy displacement by a non-Newtonian fluid in porous media according to the Barree-Conway model. Adv. Geo-energ. Res. 2017, 1(2): 74-85.

Ji, W., Song, Y., Jiang, Z., et al. Fractal characteristics of nano-pores in the Lower Silurian Longmaxi shales from the Upper Yangtze Platform, south China. Mar. Pet. Geol. 2016, 78: 88-98.

Keller, L.M., Holzer, L., Wepf, R., et al. 3-D geometry and topology of pore pathways in Opalinus 8 clay: Implications for mass transport. Appl. Clay Sci. 2011, 52(1-2): 85-95.

Li, J., Yu, T., Liang, X., et al. Insights on the gas permeability change in porous shale. Adv. Geo-energ. Res. 2017a, 1(2): 69-73.

Lin, D., Wang, J., Yuan, B., et al. Review on gas flow and recovery in unconventional porous rocks. Adv. Geo-energ. Res. 2017, 1(1): 39-53.

Liu, Y., Liu, Y., Sun, L., et al. Multiscale fractal characterization of hierarchical heterogeneity in sandstone reservoir, Fractals 2016, 24(3): 1650032.

Li, X., Liang, J., Xu, W., et al. The new method on gas-water two phase steady-state productivity of fractured horizontal well in tight gas reservoir. Adv. Geo-energ. Res. 2017b, 1(2): 105-111.

Lonnes, S., Guzman-Garcia, A., Holland, R. NMR petrophysical predictions on cores. Paper SPWLA2003 Presented at SPWLA 44th Annual Logging Symposium, Galveston, Texas, 22-25 June, 2003.

Loucks, R.G., Reed, R.M., Ruppel, S.C., et al. Morphology, genesis, and distribution of nanometer-scale pores in siliceous mudstones of the Mississippian Barnett Shale. J. Sediment. Res. 2009, 79(12): 848-861.

Mai, A., Kantzas, A. An evaluation of the application of low field NMR in the characterization of carbonate reservoirs. Paper SPE77401 Presented at SPE Annual Technical Conference and Exhibition, San Antonio, Texas, 29 September-2 October, 2002.

Mandelbrot, B.B. Les objects fractals: Forme, Hasard et dimension. Flammarion, Paris, 1975.

Martin, P., Dacy, J. Effective Qv by NMR core tests. Paper SPWLA2004 Presented at SPWLA 45th Annual Logging Symposium, Noordwijk, Netherlands, 6-9 June, 2004.

Meng, M., Ge, H., Ji, W., et al. Research on the auto-removal mechanism of shale aqueous phase trapping using low field nuclear magnetic resonance technique. J. Pet. Sci. Eng. 2016, 137: 63-73.

Morrow, N.R. Physics and thermodynamics of capillary action in porous media. Ind. Eng. Chem. 1970, 62(6): 9.

Nelson, P.H. Pore-throat sizes in sandstones, tight sandstones, and shales. AAPG Bull. 2009, 93(3): 329-340.

Ross, D.J.K., Bustin, R.M. The importance of shale composition and pore structure upon gas storage potential of shale gas reservoirs. Mar. Pet. Geol. 2009, 26(6): 916-927.

Sheng, G., Su, Y., Wang, W., et al. Application of fractal geometry in evaluation of effective stimulated reservoir volume in shale gas reservoirs. Fractals 2017, 25(4): 1740007.

Sheng, M., Li, G., Tian, S., et al. A fractal permeability model for shale matrix with multi-scale porous structure. Fractals 2016, 24(1): 1650002.

Sidiq, H., Amin, B., Kennaird, T. The study of relative permeability and residual gas saturation at high pressures and high temperatures. Adv. Geo-energ. Res. 2017, 1(1): 64-68.

Wang, W., Zheng, D., Sheng, G., et al. A review of stimulated reservoir volume characterization for multiple fractured horizontal well in unconventional reservoirs. Adv. Geo-energ. Res. 2017, 1(1): 54-63.

Wei, W., Xia, Y. Geometrical, fractal and hydraulic properties of fractured reservoirs: A mini-review. Adv. Geo-energ. Res. 2017, 1(1): 31-38.

Westphal, H., Surholt, I., Kiesl, C., et al. NMR measurements in carbonate rocks: Problems and an approach to a solution. Pure Appl. Geophys. 2005, 162(3): 549-570.

Yang, F., Ning, Z., Liu, H. Fractal characteristics of shales from a shale gas reservoir in the Sichuan Basin, China. Fuel 2014, 115(1): 378-384.

Yang, Y., Yao, J., Wang, C., et al. New pore space characterization method of shale matrix formation by considering organic and inorganic pores. J. Nat. Gas Sci. Eng. 2015, 27(P2): 496-503.

Yang, Y., Zhang, W., Gao, Y., et al. Influence of stress sensitivity on microscopic pore structure and fluid flow in porous media. J. Nat. Gas Sci. Eng. 2016, 36(Part A): 20-31.

Yao, Y., Liu, D., Che, Y., et al. Petrophysical characterization of coals by low-field nuclear magnetic resonance (NMR). Fuel 2010, 89(7): 1371-1380.

Yao, Y., Liu, D. Comparison of low-field NMR and mercury intrusion porosimetry in characterizing pore size distributions of coals. Fuel 2012, 95: 152-158.

Yuan, H.H., Swanson, B.F. Resolving pore-space characteristics by rate-controlled porosimetry. SPE Form. Eval. 1989, 4(1): 17-24.

Yu, B., Cai, J., Zou, M. On the physical properties of apparent two-phase fractal porous media. Vadose Zone J. 2009, 8(1): 177-186.

Yu, B., Zou, M., Feng, Y. Permeability of fractal porous media by Monte Carlo simulations. Int. J. Heat Mass Tran. 2005, 48(13): 2787-2794.

Zhang, T., Li, Z., Adenutsi, C.D., et al. A new model for calculating permeability of natural fractures in dual-porosity reservoir. Adv. Geo-energ. Res. 2017, 1(2): 86-92.

Zhang, X., Ren, D., Ren, Q. et al. The feature of the microscopic pore structure and its influence on oil displacement efficiency in Chang 6 Reservoir in Jiyuan Oilfield of Ordos Basin. Nat. Sci. Ed. 2015, 45(2): 283-290 (with Chinese abstract).

Zha, W., Yan, S., Li, D., et al. A study of correlation between permeability and pore space based on dilation operation. Adv. Geo-energ. Res. 2017, 1(2): 93-99.

Zhou, H., Perfect, E., Lu, Y., et al. Multifractal analyses of grayscale and binary soil thin section images, Fractals 2011, 19(3): 299-309.

Zou, C. Unconventional petroleum geology. Elsevier, 2013.